

NLS

NASA Technical Memorandum 82829

Tribological Properties of Sintered Polycrystalline and Single Crystal Silicon Carbide

(NASA-TM-82829) TRIBOLOGICAL PROPERTIES OF
SINTERED POLYCRYSTALLINE AND SINGLE CRYSTAL
SILICON CARBIDE (NASA) 28 p HC A03/MF A01

CSCL 11G

N82-24343

Unclas

63/27

09906

Kazuhisa Miyoshi and Donald Buckley
Lewis Research Center
Cleveland, Ohio

and

M. Srinivasan
Carborundum
Niagara Falls, New York



Prepared for the
Eighty-Fourth Annual Meeting of the American Ceramic Society
Cincinnati, Ohio, May 2-5, 1982



RECON CHECKED FOR A # 6482

TRIBOLOGICAL PROPERTIES OF SINTERED POLYCRYSTALLINE AND
SINGLE CRYSTAL SILICON CARBIDE

Kazuhisa Miyoshi and Donald H. Buckley
National Aeronautics and Space Administration
Lewis Research Center
Cleveland, Ohio 44135

and

M. Srinivasan
Carborundum
P.O. Box 832
Niagara Falls, New York 14302

ABSTRACT

Tribological studies and X-ray photoelectron spectroscopy analyses were conducted with sintered polycrystalline and single crystal silicon carbide surfaces in sliding contact with iron at various temperatures to 1500° C in a vacuum of 30 nPa. The results indicate that there is a significant temperature influence on both the friction properties and the surface chemistry of silicon carbide.

The main contaminants on the as-received sintered polycrystalline silicon carbide surfaces are adsorbed carbon, oxygen, graphite and silicon dioxide. The surface revealed a low coefficient of friction. This is believed to be due to the presence of the graphite on the surface. At temperatures of 400° to 600° C graphite and copious amount of silicon dioxide were observed on the polycrystalline silicon carbide surface in addition to silicon carbide. At 800° C, the amount of the silicon dioxide decreased rapidly and the silicon carbide-type silicon and carbon peaks were at a maximum intensity in the XPS spectra. The coefficients of friction were high in the temperature range of 400° to 800° C. Small amounts of carbon and oxygen contaminants were observed on the as-received single crystal silicon carbide surface below 250° C. Silicon carbide-type silicon and carbon peaks were

seen on the silicon carbide in addition to very small amount of graphite and silicon dioxide at temperatures of 450° to 800° C. The coefficients of friction were high over entire temperature range to 800° C. Above 800° C, the concentration of the graphite increases rapidly on both polycrystalline and single crystal silicon carbide surfaces, whereas those of the silicon carbide-type silicon and carbon peaks decrease rapidly. The presence of graphite is accompanied by a significant decrease in friction.

INTRODUCTION

Silicon carbide has been used as a wear, corrosion, oxidation, erosion, creep and fracture resistant material in high temperature technology. It is also used in stable high-temperature semiconductors.

Many studies have been reported on silicon carbide covering such subjects as single crystal growth, structure, imperfections, surfaces, thin film coatings, diffusion, electrical and optical characteristics, mechanical properties, radiation effects, and device fabrication techniques (refs. 1 to 23). The tribological properties and surface characteristics, however, such as adhesion, friction, wear and surface chemistry, of silicon carbide in contact with metals, ceramics and polymers are not clearly understood in many aspects. All technological processes of interacting surfaces in relative motion essentially depend on the tribological properties and the surface characteristics of the materials. Miyoshi and Buckley have conducted experimental studies with silicon carbide in single crystal form in order to gain a fundamental understanding of the surface characteristics of silicon carbide and its relation to adhesion and friction properties as well as its deformation and fracture behavior (refs. 24 to 31). The present study is an extension of that work to the tribological properties and surface chemistry of sintered alpha silicon carbide in the polycrystalline form.

Sintered alpha silicon carbide is a self-bonded form of silicon carbide which lends itself to fabrication of large complex shapes and advances substantially to the capability of ceramics to resist severe wear, erosion, corrosion, and thermal problems in practical applications. The sintered silicon carbide is very stable and superior to chemically bonded forms of silicon carbide. It is formed by conventional ceramic processing techniques such as cold pressing, injection molding, and extruding prior to firing. After the green forming step, silicon carbide is fired at a high temperature (1000° C in an argon atmosphere) resulting in dense, self-bonded bodies.

The objective of the present paper is to discuss the surface chemistry and the tribological properties of sintered polycrystalline and single crystal alpha silicon carbides at elevated temperatures. Polycrystalline and single crystal silicon carbide specimens were heated in a vacuum system at a pressure of 30 nPa by resistance heating to 1200° and 1500° C, respectively. The surface chemistry of silicon carbide crystals was analyzed by X-ray photoelectron spectroscopy (XPS). XPS provides a surface composition analysis and is a preferred analysis technique when electron radiation damage is of concern, since X-ray excitation causes very little radiation damage to most materials. The in situ sliding friction experiments were conducted with a sintered polycrystalline specimen and a single crystal alpha silicon carbide surface in contact with polycrystalline iron at temperatures from 23° to 1200° C. All friction experiments were conducted with loads to 0.3 N, at a sliding velocity of 5×10^{-2} mm/s, and in a vacuum of 30 nPa.

MATERIAL

The sintered polycrystalline alpha silicon carbide used in the experiments was a 98.5 to 98.7-percent-pure compound of silicon and carbon (table 1).

The single-crystal alpha silicon carbide used in the experiments was a 99.9-percent-pure compound of silicon and carbon (table 2). The crystal was grown by a carbon arc method. Alpha silicon carbide has a hexagonal close-packed crystal structure with the most commonly occurring unit cell dimensions being $a = 0.30817 \text{ nm}$ and $c = 1.51183 \text{ nm}$ (ref. 3). The unit cell contains two interpenetrating, close-packed atomic arrays - one of silicon and the other of carbon displaced by one-quarter of a layer spacing along the c axis. The silicon atoms thus occupy the tetrahedral locations in the array of carbon atoms, and vice versa (refs. 4 and 5). Hence the basic unit of the structure can be considered to be a plane of a tetrahedron, arbitrarily SiC_4 or CSi_4 .

The {0001} plane was nearly parallel to the sliding surfaces examined herein. The X-ray back-reflection Laue photographs were taken to establish the exact bulk orientation of the crystals after the crystals had been polished. Specimens were within $\pm 35 \text{ m rad}$ of the low index {0001} plane. The silicon carbide samples were in the form of flat platelets. The roughness of the silicon carbide surfaces measured by surface profilometer was $0.1 \text{ }\mu\text{m}$ for the maximum height of irregularities.

The polycrystalline iron was electron-beam-zone refined and was 99.99 percent pure. The crystallite size was 300 micrometers or more. The radius of the iron pin specimen was 0.79 mm.

APPARATUS

An apparatus which is capable of measuring adhesion, load, and friction was mounted in an ultrahigh vacuum system (see fig. 1). The ultrahigh vacuum system contained an X-ray photoelectron spectrometer. The major components shown in the figure include the electron energy analyzer, the X-ray

source and the ion gun used for ion sputter etching. The X-ray source contains a magnesium anode.

EXPERIMENTAL PROCEDURE

Specimen Preparation and Heating

The silicon carbide specimens were heated by resistance heating by applying tantalum thin-film coatings were applied to the back surfaces of eight silicon carbide crystals in a commercial radio frequency diode apparatus. The sliding surfaces of the silicon carbide specimens and the pin specimens to be used in the friction experiments were then polished and cleaned with diamond powder (3- μm diameter) and with aluminum oxide powder (1- μm diameter). The back of each specimen was attached to tantalum rods with tantalum supporting sheets. The tantalum-coated surface of the specimen was directly in contact with the rods. The power for resistance heating of silicon carbide specimen is supplied through the tantalum rods or sheets and the coated tantalum film by a precisely regulated DC output, adjustable over a wide range. The temperature of the silicon carbide surface was measured with a conventional thermocouple in direct contact with the surface of the silicon carbide specimen. The flat and pin specimens were rinsed with pure ethyl alcohol, just before being placed in the vacuum chamber. The specimens were placed in the vacuum chamber, and the system was evacuated and subsequently baked out to obtain a pressure of 30 nPa. The specimen was heated to a temperature of 80° C during baking out.

Surface treatments were then conducted in situ on the silicon carbide flat specimens in both vacuum chambers. The surface treatments included heating to a maximum temperature of 1200° or 1500° C at a pressure of 30 nPa and subsequent cooling to room temperature with the crystal in the as-received state after bake-out in the vacuum chamber. The surface of the

silicon carbide was resistance heated at various temperatures starting at 250° C. The specimen was heated for periods of 1 or 3 hours at a pressure of 30 nPa. The XPS spectra of the specimen were obtained before and after heating. XPS analyses after cooling to room temperature were conducted on these specimens in the same manner as those at 250° C. Heating times varied from 1 or 3 hours at each temperature in a vacuum of 30 nPa.

Ion Sputter Etching

The pin specimens were ion sputter cleaned. To conduct depth profiling of the silicon carbide flat surface, the silicon carbide flat specimen was also ion sputter etched. Ion sputter etching was performed with a beam energy of 3000 electron volts at 20 milliamperes beam current with an argon pressure of 8×10^{-3} Pa or 7×10^{-4} Pa for a predetermined sputter etching time. The ion beam was continuously rastered over the specimen surface. After sputter etching, the system was reevacuated to a pressure of 30 nPa or lower.

X-ray Photoelectron Spectroscopy

To obtain reproducible results, a strict standardization of the order and time of recording was used. The instrument was calibrated regularly. The analyzer calibration was determined assuming the binding energy for the gold 4f 7/2 peak to be 13.4 eV (83.8 eV), that is, the Au 4f 7/2 level was used as the reference line. All survey spectra, scans of 1000 or 1100 eV, were taken at a pass energy of 50 eV providing an instrumentation resolution of 1 eV at room temperature. The Mg K α X-ray was used with an X-ray source power of 400 W (10 kV - 40 mA). The narrow scans of individual peaks are just wide enough to encompass the peaks of interest and were obtained with a pass energy of 25 eV at room temperature.

To determine accurately the energy and the shape of peaks, spectra were recorded several times. The resolution of the spectral peak was 1.5 eV full

width. The energy resolution was 2 percent of the pass energy, that is, 0.5 eV. The peak maxima could be located to ± 0.1 eV. The reproducibility of peak height was good, and the probable error in the peak heights ranged from ± 2 to ± 8 percent. The peak ratios were generally good to ± 10 percent or less.

Friction Experiments

In situ friction experiments were conducted with the as-received, and surface-treated silicon carbide specimens over a temperature range from room to a maximum of 1200° C in order to not exceed the melting point of iron (1535° C). A load of 0.2 N was applied to the pin-flat contact by deflecting the beam, as shown in figure 1. The calculated mean contact pressure at a 0.2 N load with a 0.79-mm-radius iron pin in contact with silicon carbide would nominally be 0.8 GPa at room temperature. To obtain consistent experimental conditions, the time in contact before sliding was 30 seconds. Both load and friction forces were continuously monitored during a friction experiment. Sliding velocity was 5×10^{-2} mm/s with a total sliding distance of 2 to 3 mm. The values of coefficients of friction reported herein were obtained by averaging 3 to 5 measurements. The standard deviations of the measured values are within 2 to 4 percent of the mean value.

RESULTS AND DISCUSSION

X-Ray Photoelectron Spectroscopy

Sintered Polycrystalline Silicon Carbide. - The XPS survey spectra of the polycrystalline silicon carbide surfaces obtained before sputter cleaning revealed oxygen peaks, in addition to silicon and carbon peaks. The crystals were in the as-received state after it had been baked out at a temperature of 80° C in a vacuum system of 30 nPa. The XPS spectra of Si_{2p} , C_{1s} and O_{1s} obtained from narrow scans on the polycrystalline silicon carbide surfaces

are presented in figure 2. The as-received crystal (after bake-out) was heated at various temperatures in a 30 nPa vacuum. The temperatures given in figure 2 were the highest temperatures to which the crystal had been heated. All the XPS spectra were taken at room temperature after bake out and heating. The results of figure 2 show a significant influence of temperature on the silicon carbide surface characteristics.

The photoelectron emission lines for Si_{2p} of the silicon carbide are primarily split asymmetrically into doublet peaks at temperatures from room to 600° C (fig. 2(a)). The doublet peaks at 100.4 and 103.4 eV are due to distinguishable kinds of silicon compounds, which are silicon carbide and silicon dioxide, respectively. Above 600° C, the Si_{2p} photoelectron peak associated with silicon carbide is exclusively seen in the spectra.

The C_{1s} photoelectron emission lines of the silicon carbide at temperatures from room to 400° C include primarily three distinguishable kinds of peaks associated with (1) adsorbed carbon contaminant, (2) graphite, and (3) silicon carbide (fig. 2(b)). The C_{1s} photoelectron emission lines at temperatures from 600° to 1200° C are split asymmetrically into doublet peaks associated with graphite and silicon carbide.

The O_{1s} photoelectron emission lines primarily include silicon dioxide O_{1s} peaks as well as small concentrations of adsorbed oxygen contaminants at temperatures from room to 800° C. At temperatures of 1000° and 1200° C the O_{1s} peaks are negligible.

In addition, a change in the vertical height of the peaks is observed in figure 2. There are distinct influences of temperature on the Si_{2p} , C_{1s} , and O_{1s} concentrations. The heights of the Si_{2p} (silicon carbide and silicon dioxide), C_{1s} (adsorbed carbon contaminant, graphite, and silicon carbide), O_{1s} (adsorbed oxygen contaminant and silicon dioxide) on

the silicon carbide surfaces are plotted as a function of temperature in figure 3. The trend of concentration of the Si_{2p} related to the silicon carbide is similar to that of C_{1s} related to carbide over the entire temperature range of from room to $1200^{\circ}C$, as shown in figure 3(a). The heights of Si_{2p} and C_{1s} , which are related to the silicon carbide, increase linearly with increasing temperature to $800^{\circ}C$, and then decrease with increasing temperature above $800^{\circ}C$. The carbon contaminant C_{1s} peak height decreases rapidly with increasing temperature to $400^{\circ}C$, as shown in figure 3(b). The graphite C_{1s} peak is present even on the as received silicon carbide surface. This is a distinguishing feature of the sintered polycrystalline silicon carbide, because the graphite C_{1s} peak is absent on the as-received single crystal silicon carbide as will be shown in figure 4. In figure 3(b), the graphite C_{1s} peak height is relatively constant at temperatures to $400^{\circ}C$. Above $400^{\circ}C$ the graphite C_{1s} peak height increases with increasing temperature. Large graphite peaks are observed at temperatures of 1000° and $1200^{\circ}C$. In other words, the surface of silicon carbide is covered with a graphite layer.

The trend of the height of O_{1s} peak related to silicon dioxide is similar to that of Si_{2p} associated with silicon dioxide, as shown in figure 3(c). The peak heights of silicon dioxide Si_{2p} and O_{1s} obtained from the silicon carbide surface increase with increasing temperature to $600^{\circ}C$. Above $600^{\circ}C$ they decrease rapidly with increasing temperature. The amount of the silicon dioxide present on the polycrystalline silicon carbide was a few times more than that on the single crystal silicon carbide.

Single Crystal Silicon Carbide. - Figure 4 presents the XPS peak heights of the Si_{2p} , C_{1s} and O_{1s} on the single crystal silicon carbide surfaces as a function of a preheating temperature of $1500^{\circ}C$. An adsorbed

carbon contaminant on the as received single crystal silicon carbide surface was evident as well as a very small amount of oxygen contaminant.

The concentration of silicon carbide Si_{2p} and C_{1s} on the single crystal silicon carbide surface increases with increasing temperature to $800^{\circ}C$, and above $800^{\circ}C$ it decreases with increasing temperature, as shown in figure 4(a). Large Si_{2p} and C_{1s} peaks associated with silicon carbide are distinguished and are at a maximum intensity at the temperature $800^{\circ}C$.

The peak heights of silicon dioxide Si_{2p} and O_{1s} remains relatively very low at temperatures of room to $1500^{\circ}C$ (fig. 4(a)). They are almost negligible at temperatures of 800° to $1500^{\circ}C$. The amount of silicon dioxide on the single crystal silicon carbide was much less than that on the sintered polycrystalline silicon carbide, as already mentioned above.

The carbon contaminant C_{1s} peak height decreases with increasing temperature and is negligible above $400^{\circ}C$, as shown in figure 4(b). The graphite C_{1s} peak was absent at temperatures from room to $250^{\circ}C$. At temperatures of 400° to $800^{\circ}C$ the graphite peak height remains low. At $900^{\circ}C$ the amount of graphite increases rapidly and further the graphite peak height increases in intensity with increasing temperature to $1500^{\circ}C$.

A very large graphite C_{1s} peak is observed on the silicon carbide surface at temperatures of $1000^{\circ}C$ and above. Therefore, the surface of silicon carbide is covered with a graphite layer above $1000^{\circ}C$.

A comparison of the XPS results obtained from sintered polycrystalline and single crystal silicon carbide surfaces preheated to various temperatures have generally the same surface chemical conditions as those of the as-received sintered polycrystalline silicon carbide with two major exceptions. The two exceptions are: (1) the amount of silicon dioxide over the

entire temperature range examined herein and (2) the presence of graphite at temperatures below 400° C.

The amount of the silicon dioxide present on the single crystal silicon carbide was a few times less than that on the sintered polycrystalline silicon carbide over the entire temperature range examined. The graphite peaks were negligible on the single crystal silicon carbide surface, while those on the polycrystalline silicon carbide surface were quite visible. It is anticipated from these results that the friction properties of the polycrystalline silicon carbide would be different from those of the single crystal silicon carbide.

Depth Profile of Graphitized Surface

A typically complete elemental depth profile for the single crystal silicon carbide surface preheated to 1500° C was obtained as a function of sputtering time and is presented in figure 5. The graphite peak decreases rapidly in the first 30 minutes of sputtering, and thereafter it gradually decreases with an increase in the sputtering time to about 18 hours. After 18 hours the graphite peak height does not change much with sputtering time. On the other hand, the silicon carbide-Si_{2p} and C_{1s} peak heights increase gradually with increasing sputtering times to 20 hours.

Ellipsometric measurements were conducted with two different {0001} faces of the silicon carbide crystals, one which consisted of silicon atoms {0001} and the other which consisted of carbon atoms {0001} at temperatures above 1200° C (ref. 32). In 1 hour of heating at 1300° C the layer, which consists of carbon (graphite), on the C-face grows to about 100 nm, whereas the layer on the Si-face did not grow thicker than 10 nm even with longer heating.

The silicon carbide {0001} surfaces used in this investigation consisted of both silicon atoms and carbon atoms because etching of the silicon carbide surface in molten salt $1\text{NaF} + 2\text{KCO}_3$ gives both a smooth surface for the Si-face and a rough surface for the C-face. The apparent thickness of the layer, which consists of graphite and is produced by heating above 1200°C for 1 hour, is about 100 nm (1000 Å), and it is equivalent to a depth of a layer sputter etched for about 18 hours shown in figure 5.

The graphitization behavior in the outermost surficial layer is believed to be as follows. The analysis depth with AES is of the order of 1 nm or less and an elemental concentration as low as 0.1 percent of a monolayer can be detected and identified. The analysis depth with XPS is of the order of 2 nm or less, and the ultimate sensitivity is sufficient to allow fractions of a monolayer to be detected and identified. Therefore, the outermost surficial layer, which consists of mostly graphite and very little silicon, on the silicon carbide surface is concluded to be of the order of 1 nm. This estimation is consistent with the proposition of Bommel, et al. (ref. 7), that is the collapse of the carbon of three successive silicon carbide layers is the most probable mechanism for the initial stages of the graphitization of silicon carbide basal planes.

FRICITION

Sliding friction experiments were conducted with sintered polycrystalline and single crystal silicon carbide in contact with iron in vacuum. Friction-force traces resulting from such sliding experiments were generally characterized by a stick-slip behavior (ref. 33). All the coefficients of friction reported in figures 6 and 7 are static values. The coefficient of static friction μ is defined: $\mu = F_1/W$, where F_1 is the friction force at which the first break, that is, first motion is observed in the

friction-force trace and W is the normal load. The kinetic friction properties of silicon carbide in sliding contact with iron were generally of the same magnitude as those of the static friction. The kinetic friction is also defined: $\mu_k = F/W$, where F is the friction force determined by averaging the heights of maximum peaks in the friction-force trace, and W is the normal load.

The coefficient of friction of polycrystalline and single crystal silicon carbide {0001} surfaces in contact with iron as a function of sliding temperatures is indicated in figures 6 and 7, respectively. The iron rider was sputter cleaned with argon ions. Both silicon carbide specimens were in the as-received state after they had been baked out in the vacuum system. The specimens were then heated to the sliding temperature before the friction experiment was initiated. In figure 6 the coefficient of friction remains low below 250° C. The low friction can be associated with the presence of graphite, as anticipated above. The coefficient of friction increases rapidly with increasing temperature at the temperature 400° C, and remains high in the range of 400° to 800° C. The rapid increase in friction at 400° C can be related to (1) the presence of increased silicon dioxide, (2) increased adhesion, and (3) increased plastic flow in the area of contact. It is possible that the iron breaks through the graphite layer on the as-received sintered silicon carbide and comes directly in contact with the silicon carbide. When this occurs, there can be very strong adhesive bonding at the sliding interface. Above 800° C the coefficient of friction decreases rapidly with an increase of temperature. The rapid decrease in friction above 800° C correlates with the graphitization of the silicon carbide surface, as already discussed.

For single crystal silicon carbide the coefficient of friction increases slightly with increasing temperature at temperatures below 400° C, as shown in figure 7. Above 400° C, the coefficient of friction decreased with an increase in temperature in the range 400° to 600° C. The general decrease in friction at these temperatures is due to the gradual removal of the contaminant oxygen from the surface as supported by the XPS spectral data. The coefficient of friction increased with increasing temperature in the range of 600° to 800° C. The increase in friction at these temperatures can be associated with increased adhesion and increased plastic flow in the area of contact. Above 800° C the coefficient of friction decreases rapidly with an increase of temperature. The rapid decrease in friction above 800° C correlates with the graphitization of the silicon carbide surface as already discussed.

Thus, the low friction at the high temperatures (above 800° C) appears to correlate with the graphitization of the silicon carbide surface. The coefficients of friction on the single crystal and sintered polycrystalline silicon carbide surfaces at high temperatures are nearly the same as those on pyrolytic graphite in sliding contact with iron in a vacuum (ref. 34).

METAL TRANSFER

An inspection of the sintered polycrystalline and single-crystal silicon carbide surfaces after sliding contact with iron revealed transfer of iron to silicon carbide. Figure 8 presents scanning electron micrographs at the beginning of wear tracks on the as-received surfaces of silicon carbide generated by a single pass of the iron at room temperature. It is obvious from figure 8 that the iron transfers to the silicon carbide even with single pass sliding. The higher the sliding temperature, the more the extent of the metal transfer produced to the ceramic surface (ref. 31).

FRACTURE WEAR

The sliding of iron on a silicon carbide surface at room and elevated temperatures results in formation of cracks and fracture pits in the silicon carbide surface. The fracture wear occurs very locally and in very small areas in the sliding contact region.

Two of the present authors have observed multiangular and spherical wear particles of single crystal silicon carbide when silicon carbide was in sliding contact with metals or nonmetals (refs. 25 and 30). It was suggested that wear debris and fracture pits of silicon carbide were produced by two mechanisms. The first involves the formation of a multiangular-shaped fracture along the {0001}, {1010}, and {1120} cleavage planes under the Hertzian stress field or local inelastic deformation zone, and the second involves the formation of a spherical-shaped fracture along the circular or spherical stress trajectories under the inelastic deformation zone (ref. 30).

Figure 9 presents a scanning electron micrograph of the wear track on the polycrystalline sintered silicon carbide surface, where the wear track is generated by single pass sliding of the iron rider. The wear track has microfracture pits in it. The microfracture pits, where the wear debris particles were ejected, reveals that the fracturing is the result of surface and subsurface fracture.

CONCLUSIONS

The following conclusions are drawn from the data presented herein:

1. There is a significant temperature influence on both the surface chemistry and tribological properties of silicon carbide.
2. The principal contaminants on the as-received sintered polycrystalline silicon carbide surfaces are adsorbed carbon and oxygen, graphite and silicon dioxide. The adsorbed carbon contaminants disappear on heating to

400° C. Above 400° C, graphite and silicon dioxide are primarily seen on the silicon carbide surface in addition to the silicon carbide. The amount of silicon dioxide present on the silicon carbide decreases rapidly with increasing temperature in the range of 600° to 800° C. At 800° C, the silicon carbide-Si_{2p} and C_{1s} peaks are at maximum intensity as determined by the XPS spectra. Above 800° C, graphite concentration increases rapidly with an increase in temperature on the silicon carbide surface. The surface of silicon carbide graphitizes at temperatures of 1000° to 1200° C.

3. The principal contaminants on the as-received single crystal silicon carbide surface is adsorbed carbon, oxygen and silicon dioxide. The amount of the silicon dioxide present on the single crystal silicon carbide is less than that on the sintered polycrystalline silicon carbide. The adsorbed carbon contaminants disappear on heating to 400° C. Above 400° C, graphite and silicon carbide are primarily seen on the silicon carbide surface. At 800° C, the silicon carbide-Si_{2p} and C_{1s} peaks are at an maximum intensity. Above 800° C, the graphite concentration increases rapidly with an increase in temperature, while the silicon carbide concentration decreases rapidly in intensity from the silicon carbide surface.

4. The general temperature dependent trend of the coefficient of friction for sintered polycrystalline silicon carbide is similar to that for single crystal silicon carbide in the range of 400° to 1200° C. The coefficients of friction were high at temperatures of 400° to 800° C. Above 800° C, coefficients of friction was dramatically lower because of the presence of the graphite layer on the surface of the silicon carbide.

The surface of the as-received polycrystalline silicon carbide at room temperature and 250° C revealed a low coefficient of friction. This is be-

lieved to be due to the existence of graphite of the silicon carbide surface during fabrication.

5. Iron transferred to the surface of silicon carbide in even a single pass of sliding.

REFERENCES

1. J. R. O'Connor and J. Smiltens, eds., *Silicon Carbide, a High Temperature Semiconductor*. Pergamon Press, New York, 1960.
2. R. C. Marshall, J. W. Faust, Jr., and C. E. Ryan, eds., *Silicon Carbide - 1973, Proceedings of the Third International Conference*, University of South Carolina Press, Columbia, S.C., 1974.
3. A. Taylor, and D. S. Laidler, "Formation and Crystal Structure of Silicon Carbide," *Brit. J. Appl. Phys.*, 1 (7) 174-181 (1950).
4. A. W. Hull, "The Crystal Structure of Carborundum," *Phys. Rev.*, 13 292-295 (1919).
5. H. Ott, "Structure of Carborundum (SiC)," *Z. Krist.*, 61 515-531 (1925); and "The Lattice of Carborundum Type I," *Z. Krist.*, 62 201-217 (1926).
6. D. V. Badami, "X-Ray Studies of Graphite Formed by Decomposing Silicon Carbide," *Carbon*, 3 (1) 53-57 (1965).
7. A. J. Van Bommel, J. E. Crombeen, and A. Van Tooren, "LEED and Auger Electron Observations of the SiC (0001) Surface," *Surf. Sci.*, 48 (2) 463-472 (1975).
8. S. Amelinckx, G. Strumane, and W. W. Webb, "Dislocations in Silicon Carbide," *J. Appl. Phys.*, 31 (8) 1359-1370 (1960).
9. O. O. Adewoye, G. R. Sawyer, J. W. Edington, and T. F. Page, "Structural Studies of Surface Deformation in MgO, SiC and Si₃N₄," Cambridge University, England, Ad-A008993, Oct. 1974.

10. D. P. H. Hasselman and H. D. Batha, "Strength of Single Crystal Silicon Carbide," Appl. Phys. Letters, 2 (6) 111-113 (1963).
11. R. D. Carnahan, "Elastic Properties of Silicon Carbide." J. Am. Ceram. Soc., 51 (4) 223-224 (1968).
12. J. A. Coppola and R. C. Bradt, "Measurement of Fracture Surface Energy of Silicon Carbide," J. Am. Ceram. Soc., 55 (9) 455-460 (1972).
13. P. T. B. Shaffer, "Effect of Crystal Orientation on Hardness of Silicon Carbide," J. Amer. Ceram. Soc., 47 (9) 466 (1964).
14. C. A. Brookes and M. Imai, in *Special Ceramics 1964*, pp. 259-268. "The Frictional Properties of Silicon Nitride and Silicon Carbide," Edited by P. Popper, Academic Press, New York, 1965.
15. R. Komanduri and M. C. Shaw, "Attritious Wear of Silicon Carbide," J. Eng. Ind., 98 (4) 1125-1134 (1976).
16. K. Niihara, "Slip Systems and Plastic Deformation of Silicon Carbide Single Crystals at High Temperatures," J. Less-Common Met., 65 (1) 155-166 (1979).
17. O. O. Adewoye, "Frictional Deformation and Fracture in Polycrystalline SiC and Si₃N₄," Wear, 70 37-51 (1981).
18. J. L. Routbort, R. O. Scattergood, and A. P. L. Turner, "The Erosion of Reaction-Bonded SiC," Wear, 59 (1) 363-375 (1980).
19. A. Guivarc'h, J. Richard, M. LeContellec, E. Ligeon, and J. Fontenille, "Hydrogen Content of Amorphous Silicon Carbide Prepared by Reactive Sputtering: Effects on Films Properties," J. Appl. Phys. 51 (4) 2167-2174 (1980).
20. S. K. Lilov, Yu. N. Tairov, and V. F. Tsvetkov, "Investigation of Nitrogen Solubility Process in Silicon Carbide," Krist. Techn., 14 (1) 111-116 (1979).

21. R. A. Causey, J. D. Fowler, C. Ravanbakht, T. S. Elleman, and K. Verghese, "Hydrogen Diffusion and Solubility in Silicon Carbide," J. Am. Ceram. Soc., 61 (5-6) 221-225 (1978).
22. W. Bocker and H. Hausner, "The Influence of Boron and Carbon Additions on the Microstructure of Sintered Alpha Silicon Carbide," Powder Metall. Int., 10 (2) 87-89 (1978).
23. P. Popper and D. G. S. Davies, "The Preparation and Properties of Self-Bonded Silicon Carbide," Powder Metall., 8 113-127 (1961).
24. K. Miyoshi and D. H. Buckley, "Friction, Deformation and Fracture of Single-Crystal Silicon Carbide," ASLE Trans., 22 (1) 79-90 (1979).
25. K. Miyoshi, and D. H. Buckley: "Friction and Fracture of Single-Crystal Silicon Carbide in Contact with Itself and Titanium," ASLE Trans., 22 (2) 146-153 (1979).
26. K. Miyoshi and D. H. Buckley, "Friction and Wear Behavior of Single-Crystal Silicon Carbide in Sliding Contact with Various Metals," ASLE Trans., 22 (3) 245-256 (1979).
27. K. Miyoshi and D. H. Buckley, "The Friction and Wear of Metals and Binary Alloys in Contact with an Abrasive Grit of Single-Crystal Silicon Carbide," ASLE Trans., 23 (4) 460-472 (1980).
28. K. Miyoshi and D. H. Buckley, "Tribological Properties of Silicon Carbide in Metal Removal Process," NASA TM-79238, 1980.
29. K. Miyoshi and D. H. Buckley, "The Adhesion, Friction, and Wear of Binary Alloys in Contact with Single-Crystal Silicon Carbide," J. Lubr. Technol., 103 (2) 169-322 (1981).
30. K. Miyoshi and D. H. Buckley, "The Generation and Morphology of Single-Crystal Silicon Carbide Wear Particles Under Adhesive Conditions," Wear, 67 (3) 303-319 (1981).

31. K. Miyoshi and D. H. Buckley, "Tribological Properties and Surface Chemistry of Silicon Carbide at Temperatures to 1500° C," ASLE Preprint No. 81-LC-5A-1, 1981.
32. F. Meyer and G. J. Loya, "Ellipsometry Applied to Surface Problems—Optical Layer Thickness Measurement," Acta Electron., 18 33-38 (1975).
33. K. Miyoshi and D. H. Buckley, "Changes in Surface Chemistry of Silicon Carbide (0001) Surface with Temperature and Their Effect on Friction," NASA TP-1756, November 1980.
34. D. H. Buckley and W. A. Brainard, "Friction and Wear of Metals in Contact with Pyrolytic Graphite," Carbon, 13 (6) 501-508 (1975).

TABLE 1. - COMPOSITION DATA, HARDNESS, AND FRACTURE TOUGHNESS OF SINTERED POLYCRYSTALLINE ALPHA SILICON CARBIDE

(a) Composition (at.%)

SiC	Fe	B	Hg	Mn	Ni	Al	Ti	V	Cu	Zr	Ca
Matrix (98.5 to 98.7)	0.4	0.6	0.01	0.004	0.004	0.06	0.01	0.001	0.001	0.01	0.04

(b) Hardness and surface fracture toughness

Vickers hardness number	Fracture toughness K_{Ic} (MPa $m^{1/2}$)
3435±122 (33.65±1.20 GPa)	4.06±0.34

TABLE 2. - COMPOSITION DATA, CRYSTAL STRUCTURE, AND HARDNESS OF SINGLE CRYSTAL ALPHA SILICON CARBIDE

(a) Composition^a

Si	C	O	B	P	Others
66.6%	33.3%	<500 ppm	<100 ppm	<200 ppm	<0.1 ppm

(b) Structure

Interatomic distance		Lattice ratio, c/a
a (nm)	c (nm)	
3.0817	15.1183	4.9058
3.073	15.079	4.9059

(c) Hardness data

Plane	Direction	Knop hardness number (2.9 N)
{0001}	<1120>	2670
{0001}	<1010>	2825

^aManufacturer's analyses.

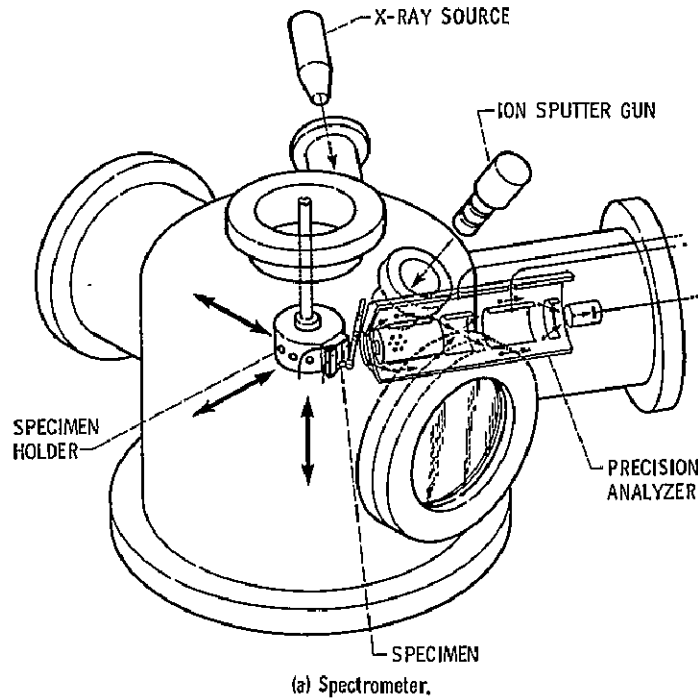


Figure 1. - Schematic representations of the X-ray photoelectron spectrometer, friction and wear apparatus and silicon carbide specimen.

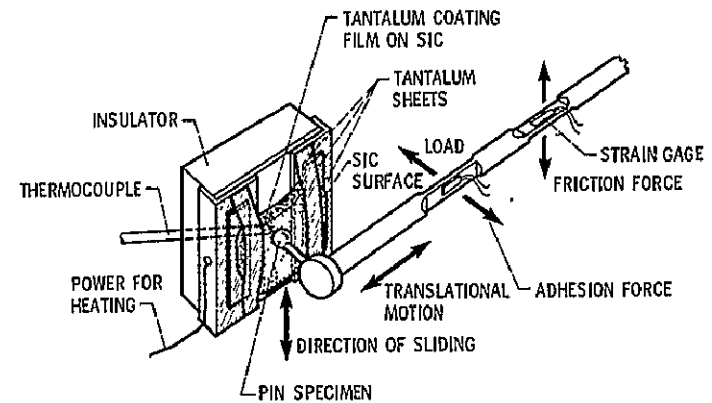


Figure 1. - Concluded.

ORIGINAL PAGE IS
OF POOR QUALITY

ORIGINAL PAGE IS
OF POOR QUALITY

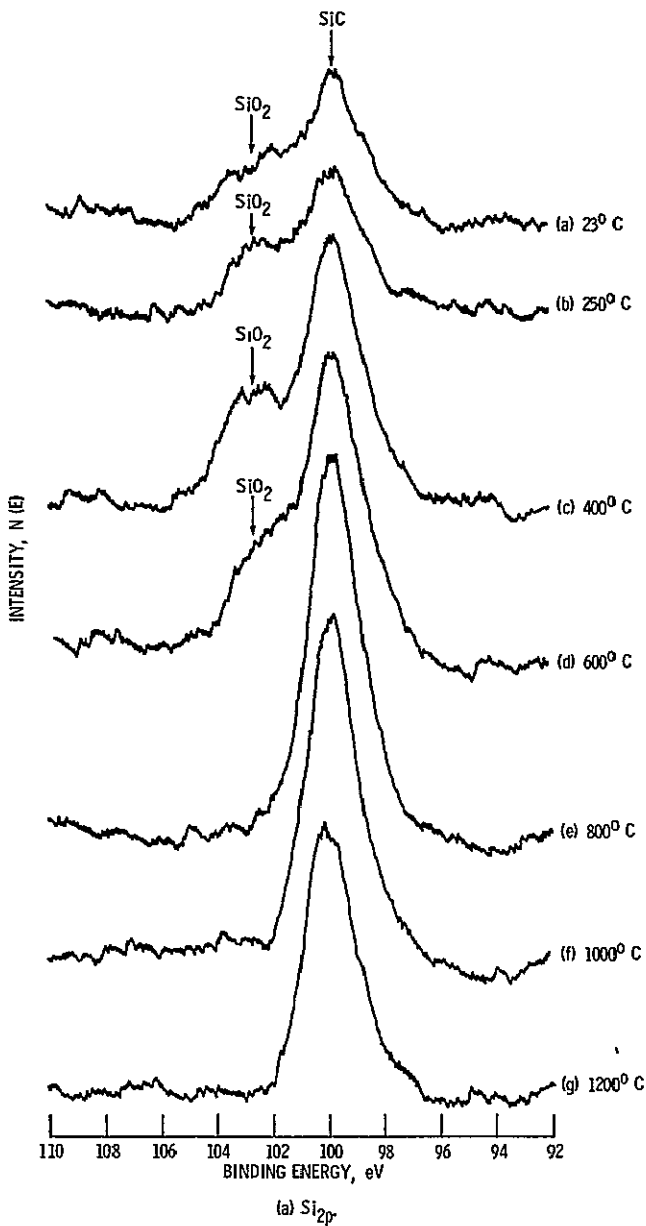


Figure 2 - Representative Si_{2p}, C_{1s} and O_{1s} XPS peaks on sintered polycrystalline silicon carbide surface preheated at various temperatures to 1200°C.

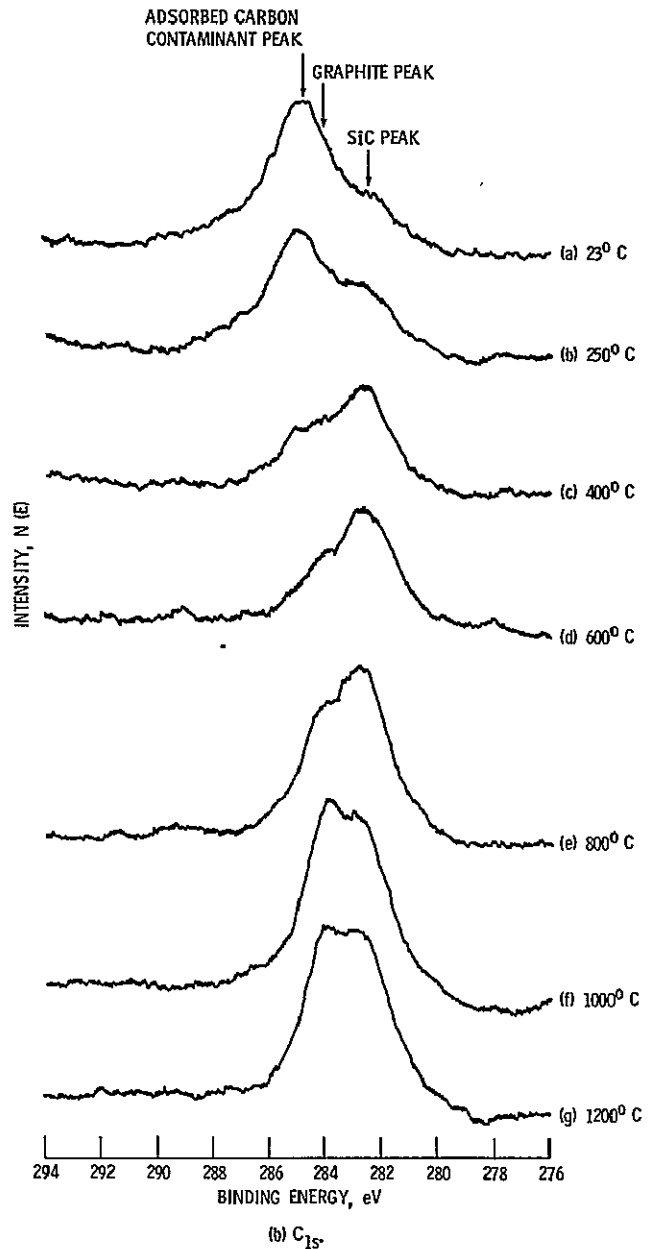
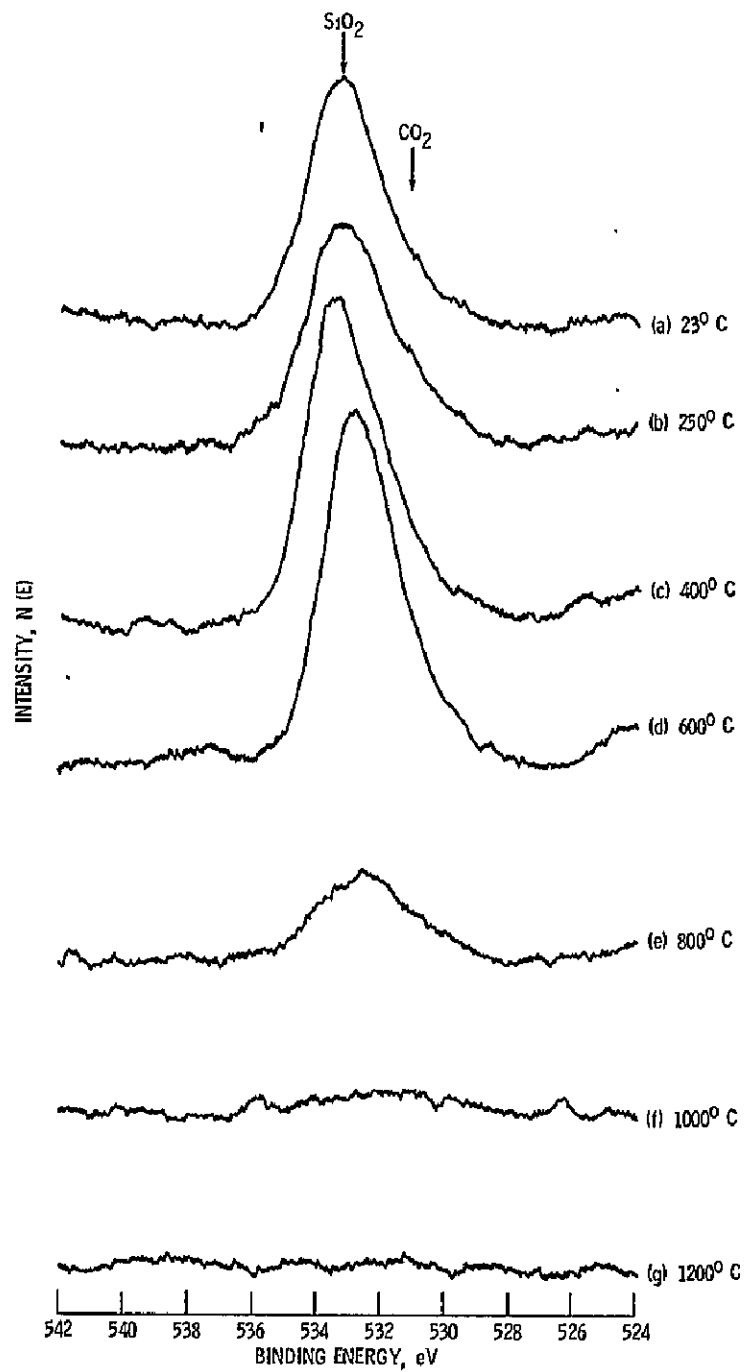
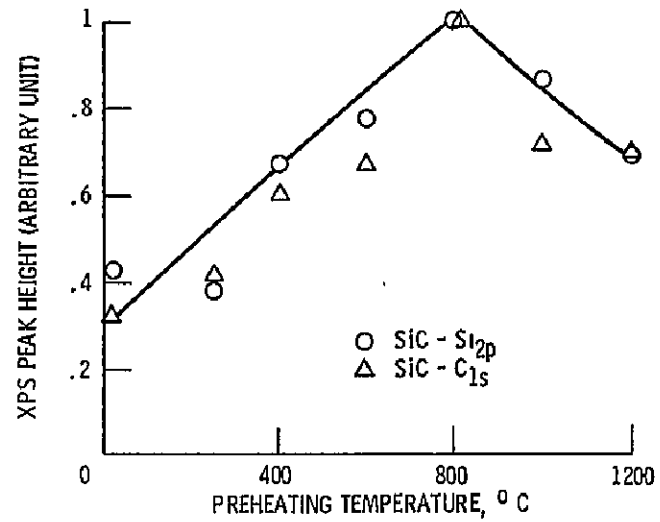


Figure 2 - Continued.



(c) O_{1s} .

Figure 2. - Concluded.

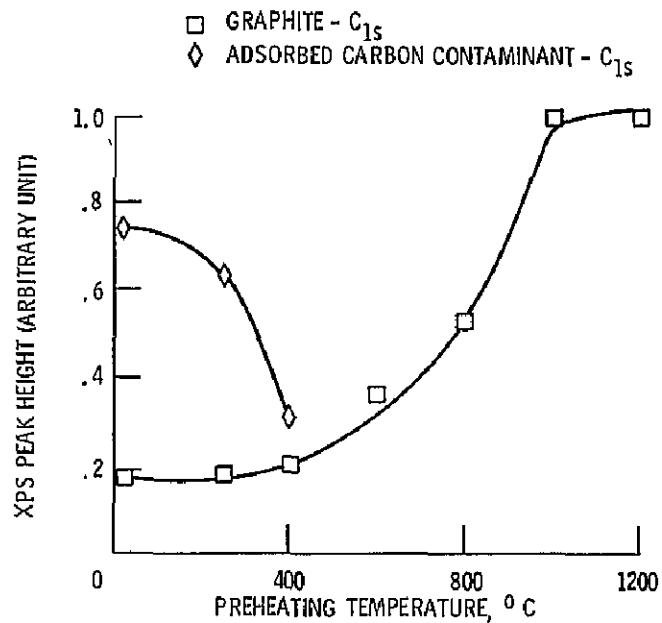


(a) $SiC - Si_{2p}$ and $-C_{1s}$ peak heights.

Figure 3. - Si_{2p} , C_{1s} and O_{1s} XPS peak heights on sintered polycrystalline silicon carbide surface preheated at various temperatures to 1200°C.

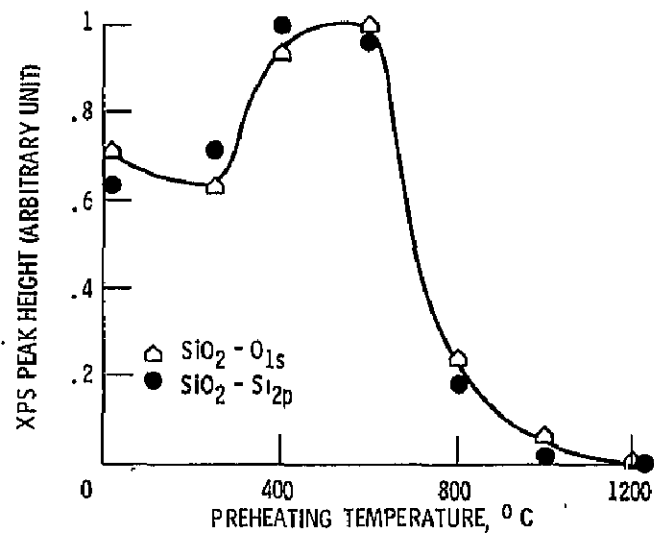
ORIGINAL PAGE IS
OF POOR QUALITY.

ORIGINAL PAGE IS
OF POOR QUALITY



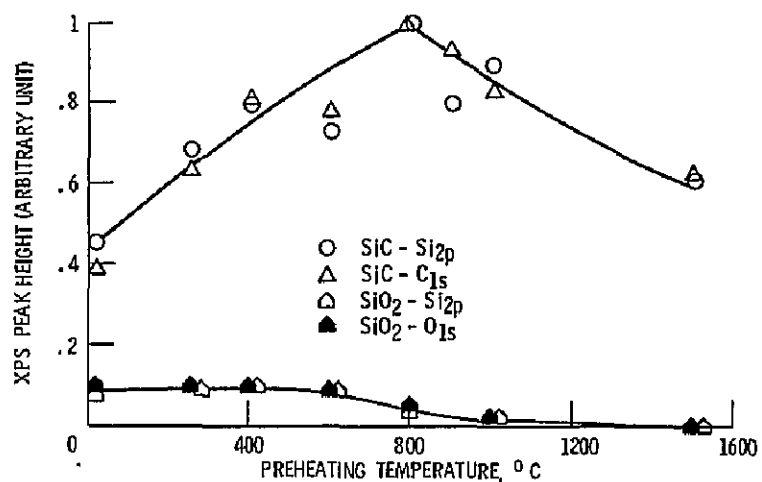
(b) Graphite - C_{1s} and adsorbed carbon contaminant - C_{1s} peak heights.

Figure 3, - Continued.



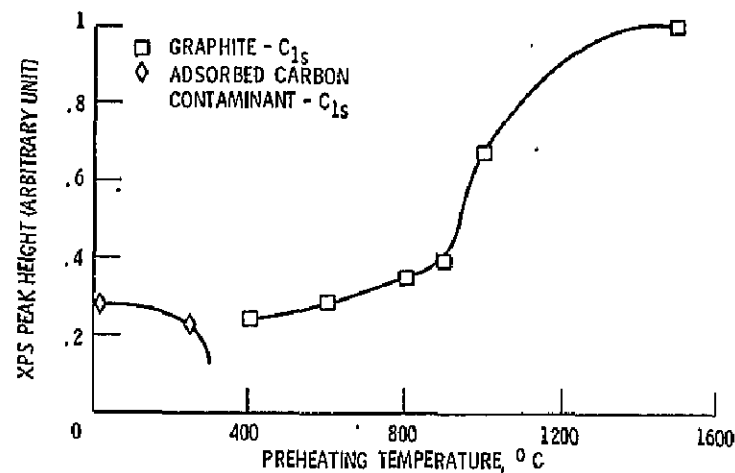
(c) SiO₂ - Si_{2p} and O_{1s} peak heights.

Figure 3, - Concluded.



(a) SiC - Si_{2p} and C_{1s}, and SiO₂ - Si_{2p} and O_{1s} peak heights

Figure 4, - Si_{2p}, C_{1s} and O_{1s} XPS peak heights on single crystal silicon carbide surface preheated at various temperatures to 1500°C.



(b) Graphite - C_{1s} and adsorbed carbon contaminant - C_{1s} peak heights.

Figure 4, - Concluded.

ORIGINAL PAGE IS
OF POOR QUALITY

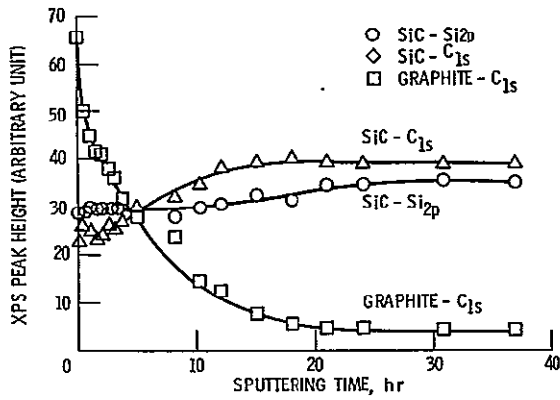


Figure 5. - Elemental depth profile of silicon carbide {0001} surface preheated to a temperature of 1500°C for 1 hour.

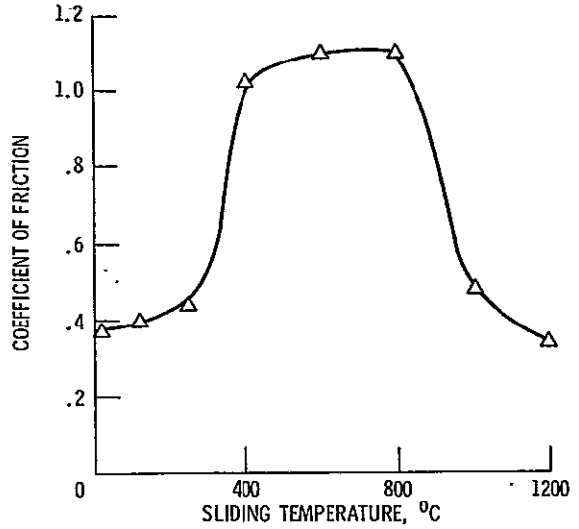


Figure 6. - Effect of temperature on coefficient of friction for sintered polycrystalline silicon carbide surface sliding against an iron rider. The iron rider was argon ion sputter cleaned before experiments. Normal load, 0.1 to 0.2N; vacuum, 30 nPa.

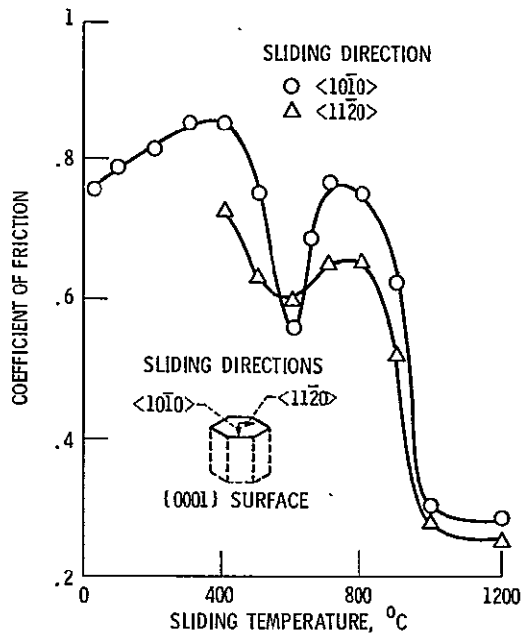


Figure 7. - Effect of temperature on coefficient of friction for silicon carbide {0001} surface sliding against an iron rider. The iron rider was argon ion sputter cleaned before experiments. Normal load, 0.2N; vacuum, 30 nPa.

ORIGINAL PAGE
BLACK AND WHITE PHOTOGRAPH



(a) SINTERED POLYCRYSTALLINE SILICON CARBIDE SURFACE; LOAD, 0.1N.



(b) SINGLE CRYSTAL SILICON CARBIDE {0001} SURFACE; SLIDING DIRECTION, $\langle 10\bar{1}0 \rangle$; LOAD, 0.2N.

Figure 8. - Iron transferred to sintered polycrystalline and single crystal silicon carbide at commencement of sliding as a result of single pass of rider at room temperature in vacuum (30 nPa).

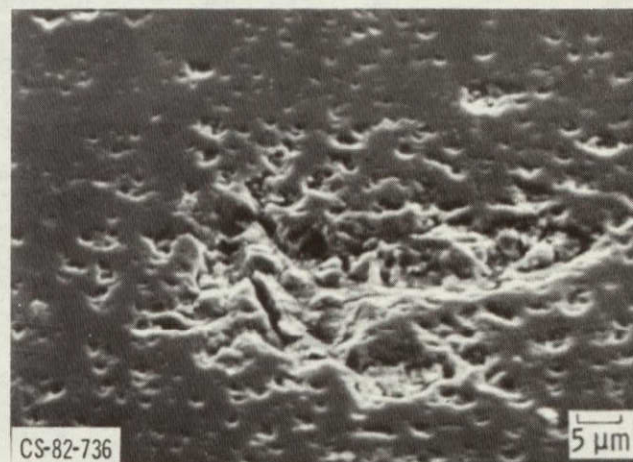


Figure 9. - Scanning electron micrographs of wear track on sintered polycrystalline silicon carbide surface. Single pass sliding of iron rider; load, 0.2N; room temperature; vacuum, 30 nPa.

ORIGINAL PAGE IS
OF POOR QUALITY

1. Report No. NASA TM-82829	2. Government Accession No.	3. Recipient's Catalog No.	
4. Title and Subtitle TRIBOLOGICAL PROPERTIES OF SINTERED POLY-CRYSTALLINE AND SINGLE CRYSTAL SILICON CARBIDE		5. Report Date	
		6. Performing Organization Code 506-53-12	
7. Author(s) Kazuhisa Miyoshi, Donald H. Buckley, and M. Srinivasan		8. Performing Organization Report No. E-1194	
		10. Work Unit No.	
9. Performing Organization Name and Address National Aeronautics and Space Administration Lewis Research Center Cleveland, Ohio 44135		11. Contract or Grant No.	
		13. Type of Report and Period Covered Technical Memorandum	
12. Sponsoring Agency Name and Address National Aeronautics and Space Administration Washington, D.C. 20546		14. Sponsoring Agency Code	
		15. Supplementary Notes Kuzuhisa Miyoshi and Donald H. Buckley, Lewis Research Center; and M. Srinivasan, Carborundum, P. O. Box 832, Niagara Falls, New York 14302. Prepared for the Eighty-fourth Annual Meeting of the American Ceramic Society, Cincinnati, Ohio, May 2-5, 1982.	
16. Abstract Tribological studies and X-ray photoelectron spectroscopy analyses were conducted with sintered polycrystalline and single crystal silicon carbide surfaces in sliding contact with iron at various temperatures to 1500 ^o C in a vacuum of 30 nPa. The results indicate that there is a significant temperature influence on both the friction properties and the surface chemistry of silicon carbide. The main contaminants on the as-received sintered polycrystalline silicon carbide surfaces are adsorbed carbon, oxygen, graphite, and silicon dioxide. The surface revealed a low coefficient of friction. This is believed to be due to the presence of the graphite on the surface. At temperatures of 400 ^o to 600 ^o C graphite and copious amount of silicon dioxide were observed on the polycrystalline silicon carbide surface in addition to silicon carbide. At 800 ^o C, the amount of the silicon dioxide decreased rapidly and the silicon carbide-type silicon and carbon peaks were at a maximum intensity in the XPS spectra. The coefficients of friction were high in the temperature range of 400 ^o to 800 ^o C. Small amounts of carbon and oxygen contaminants were observed on the as-received single crystal silicon carbide surface below 250 ^o C. Silicon carbide-type silicon and carbon peaks were seen on the silicon carbide in addition to very small amount of graphite and silicon dioxide at temperatures of 450 ^o to 800 ^o C. The coefficients of friction were high over entire temperature range to 800 ^o C. Above 800 ^o C, the concentration of the graphite increases rapidly on both polycrystalline and single crystal silicon carbide surfaces, whereas those of the silicon carbide-type silicon and carbon peaks decrease rapidly. The presence of graphite is accompanied by a significant decrease in friction.			
17. Key Words (Suggested by Author(s)) Tribology XPS SiC		18. Distribution Statement Unclassified - unlimited STAR Category 27	
19. Security Classif. (of this report) Unclassified	20. Security Classif. (of this page) Unclassified	21. No. of Pages	22. Price*

National Aeronautics and
Space Administration

Washington, D.C.
20546

Official Business
Penalty for Private Use, \$300

SPECIAL FOURTH CLASS MAIL
BOOK

Postage and Fees Paid
National Aeronautics and
Space Administration
NASA-451



NASA

POSTMASTER: If Undeliverable (Section 158
Postal Manual) Do Not Return
